On the Inclusion of Spatial Information for Spatio-Temporal Neural Networks

Rodrigo de Medrano, José L. Aznarte
Artificial Intelligence Department
Universidad Nacional de Educación a Distancia — UNED
Madrid, Spain
rdemedrano@dia.uned.es
jlaznarte@dia.uned.es

Abstract—When confronting a spatio-temporal regression, it is sensible to feed the model with any available *prior* information about the spatial dimension. For example, it is common to define the architecture of neural networks based on spatial closeness, adjacency, or correlation. A common alternative, if spatial information is not available or is too costly to introduce it in the model, is to learn it as an extra step of the model. While the use of *prior* spatial knowledge, given or learnt, might be beneficial, in this work we question this principle by comparing traditional forms of convolution-based neural networks for regression with their respective spatial agnostic versions. Our results show that the typical inclusion of *prior* spatial information is not really needed in most cases. In order to validate this counterintuitive result, we perform thorough experiments over ten different datasets related to sustainable mobility and air quality, substantiating our conclusions on real world problems with direct implications for public health and economy.

Index Terms—Neural Networks, Spatio-temporal Series, Spatial Dimension, Convolutional Neural Networks, Regression

I. INTRODUCTION

Convolutional neural networks (CNN) are well known for their ability to handle spatial data in several contexts, like images or spatial phenomena. However, in the last few years they have demonstrated to hold a good position also when dealing with temporal data. Thus, they are widely used in spatio-temporal regression problems, with outstanding behavior when coping with both spatial and temporal dimensions.

Due to its parameter structure, CNNs are usually employed when it is possible to order input data in a grid. Furthermore, they treat each location equally, learning and sharing the same weights for all spatial points. Given that it is not rare that the phenomenon under study presents the same nature all over the grid, in a wide range of applications this property is a clear advantage in order to minimize the number of parameters and calculations for learning an specific task. This leads to good performance with fewer resources compared to feedforward neural networks (FNN) and recurrent neural networks (RNN). For example, pollution and traffic regression share an approximately equivalent temporal behavior and distribution at each location (at least in a close environment), meaning that it is possible to share parameters and get a smooth approximation for these phenomena via traditional CNNs.

However, this property of CNNs (which is usually known as *equivariance*), might not always be the best deal when solving some typical problems: sometimes, although similar, treating all locations equally does not hold as a valid or acceptable hypothesis and so, learning a spatial shared-based representation might not be the best option if the system representation is not chosen carefully. In the previous example, it is obvious that different traffic sensors or pollution stations will have different properties, even though their temporal dynamic will be somehow similar. For spatio-temporal regression specifically, several proposals have been made in order to tackle this problem, but two of them stand out for their wide acceptance:

- Order the grid by Euclidean distance (from now on, just closeness) and use CNNs.
- Define the system in a graph structure and model it via graph convolutional networks (GCN).

In both cases, a classical assumption is made: closer locations have similar properties and, because of that, the shared-weights learned by the networks are more reliable. This way, the spatial dimension in CNNs keeps a low number of parameters.

However, these solutions do have some disadvantages. First, they do not completely solve the fact that each location, although related to the rest, has its own properties. Even more, although the assumption that closer locations behave similarly is usually blindly accepted, this might not hold always for real problems: not only depends on the phenomenon, but also on the temporal and spatial granularity with which the data is taken. Thus, the benefits of learning a latent representation based on sharing parameters are conditioned by the particularities of each specific problem and, contrary to popular belief, the spatial proximity between locations is not necessarily the main factor. Second, in both cases it is necessary to introduce *prior* spatial knowledge to the system, making it less 'intelligent' and more laborious to work with.

In this paper we focus on whether defining adjacency-based convolutional architectures for regression problems is as important or positive as has traditionally been assumed. To explore and contrast our hypothesis, we propose to compare a set of widely used traditional convolutional methods with their respective spatial agnostic versions. Here, the denotation "spatial agnostic" makes reference at not including specific mechanisms that exploit spatial information explicitly. By showing that no improvement is reported when using *prior* spatial knowledge, we can reject the idea that models with

a spatial bias will result systematically in better forecasters. Also, models with spatial agnostic nature can be a suitable choice when spatial information is not easily achievable or within reach.

What happens if we closely examine the temporal dimension? In multiple real applications in which this spatial agnosticism does not exactly hold, temporal equivalence between locations is more plausible: temporal distributions along spatial points might better fulfill the assumption of sharing parameters compared to the spatial dimension. This means that, while it is common to use some sort of recurrent module to model temporal relations, convolutions can be perfectly valid candidates for this work, using a lower number of parameters. Thus, sharing parameters for all locations between subsequent past timesteps in the temporal dimension might work better than in the spatial dimension.

To validate our hypothesis, we compare several models and dig deeper in the real importance of closeness relations through extensive experimentation. For this purpose, the vast field of air quality and sustainable mobility has been chosen. With a wide number of long spatio-temporal series with spatial particularities but approximately equivalent temporal dynamics (due to their relation with human behavior) and high non-linearity, it is a perfect field to corroborate our hypotheses. Since it is considered of great importance for public health and also to economy, it is potentially beneficial to have simpler and easily deployable models in this field.

The main contributions of this study are summarized as follows:

- We delve into the counterintuitive idea that including spatial relations based on closeness are not necessarily the optimal option when working with neural networks for regression in spatio-temporal problems. Concretely, we compare several traditional methodologies with their respective spatial agnostic version.
- The contribution is illustrated by tackling a variety of prediction problems related to air quality and sustainable mobility. All of them are considered of great importance and significantly complex for both spatial and temporal dimensions.
- Results show that spatial agnostic methods equal state-of-the-art models in accuracy without the need of *prior* spatial information.

The rest of the paper is organized as follows: related work is discussed in Section II, while Section III presents the methods and all needed theory for this work. Then, in Section IV we introduce our datasets, experimental design, and its properties. Section V illustrates the evaluation of the proposed architecture as derived after appropriate experimentation. Finally, in Section VI we point out conclusions from our work.

II. RELATED WORK

A. *The rise of convolutions*

Since CNNs were proposed as neural architectures [1], they have shown to handle especially well spatially-ordered data. During the last decades, this kind of neural networks have grown in importance, becoming one of the most used neural paradigms for a wide number of applications.

In the case of intrinsic 2D problems, like images, CNNs have turned out to be the option per excellence. Concretely, with [2] started a reign of CNN for computer vision problems. Not much later, the idea that weight sharing could lead to potentially suboptimal performance for some images, like portraits, was studied [3]. In the present, CNNs are widely used for this kind of problem and have been well characterized.

However, CNNs are not constrained to natural 2D systems. For example, time series seen as a 1D sequence have been handled by convolutional models with good results [4], [5]. Spatio-temporal series have growth in importance and CNNs have been well studied and are already a standard when dealing with this kind of series [6], [7]. A similar field to spatio-temporal series is video-sequence analysis, where both spatial and temporal relations need to be modeled [8]. Within this last topic, some examples in which parameter sharing is indeed highly positive can be found, as for example enhancing video spatial resolution for creating smooth results [9].

B. *Spatial dimension in spatio-temporal neural networks*

In spatio-temporal regression specifically, convolution based networks are one of the leading options too. As explained in Section I, convolution shines in a wide range of applications involving physical spatial locations. However, how this dimension is treated by the convolution has not received particular attention. Thus, we have several options that are widely used but not necessarily optimal.

For example, in traffic forecasting, defining your space as a natural grid. [10] is a good example of 2D image-to-image prediction problem in which, by using channels as timesteps and 3D kernels, spatio-temporal relations are exploited. As average traffic speeds for each road segment is used, no need to *prior* spatial information is needed and the grid arrangement is natural. However, closer areas are not necessarily more related. In [11] it is shown that the 3D convolution might work better, but the same spatial arrangements and assumptions are made.

When measurement points are directly used as an arrangement for the spatial dimension, not only it is necessary to impose same closeness supposition than before, but a special treatment is usually needed to arrange locations correctly. Some examples are [12], where the authors order traffic sensors in a 1D grid; or [13], where measurement points are ordered as 2D images.

In recent years, graphs-based networks have received increasing attention. GCNs not only have shown a very competitive performance, but a graph structure is more suitable than grids for some specific problems where relations might be non-Euclidean and directional [14]. Among the different convolutions in graphs, all of them depend heavily on an adjacency matrix which usually needs to be manually defined. This adjacency matrix is of great importance as it defines the graph relations and structure. Depending on the proposal, this matrix might be defined differently: it usually is defined by spatial closeness [15], [16], but there are no restrictions. While this freedom to define the adjacency matrix might help to avoid

the closeness assumption, it would force you to find which *prior* information may be more optimal for your particular problem. If compared to traditional CNN, GCN presents another advantage: they can naturally process information from a $K - hop$ neighborhood [17], not restricting themselves to uniquely adjacent nodes.

Temporal relations with neural networks are usually constrained to using some kind of RNNs. Although much proposals have been done, through this work we will not focus on this broad topic and we will limit its use to standards.

C. Non-locally dependent proposals

The idea that a fixed arrangement for learning spatial relations might not be the best deal is not new in spatio-temporal series forecasting. Lu et al [18] state that *"the existence of spatial heterogeneity imposes great influence on modeling the extent and degree of road traffic correlation, which is usually neglected by the traditional distance based method"*, and proposed a data-driven approach to measure these correlations. From this starting point, we can select several works that have contributed to refine and depend less on *prior* information in the spatial dimension using neural models.

By using a hierarchical clustering over the spatio-temporal data, [19] refines spatial relations. However, it uses a distance matrix in the process, introducing the aforementioned bias by closeness. In [20], a lasso methodology is used to obtain a sparse model of the system dynamics, which simultaneously identifies spatial correlation along with model parameters.

Attention mechanisms, which appeared on the deep learning scene a few years ago, are a natural way to learn relations beyond the network original assumptions. In this context, several works have used attention weights to improve performance and demonstrate the correctness of their work with both, grid structure [21] and graph structure [22]. However, [13] shows how closer locations are not necessarily more related, and depending on the problem and the characteristics of the regression, other considerations might be more important when learning spatial relations.

Closer to our work, in [23] a similar issue but with general multivariate time series forecasting is put on the table: existing methods usually fail to fully exploit latent spatial dependencies between pairs of variables and GCNs require well-defined graph structures which means they cannot be applied directly for multivariate time series where the dependencies are not known in advance. In their proposal, they construct a new model that tackles both problems. [24] focus its efforts on dealing with the fact that different spatial locations might have at some degree different dynamics by using traditional CNNs but with the introduction of learnable local inputs/latent variables and learnable local transformations of the inputs.

In the end, all these works focus its attention on solving a specific regression problem, but not delve into how the spatial dimension should be really treated. Furthermore, all these methodologies have in common the need to make their models considerably more complex in order to overcome spatial agnosticism, generally starting from usual convolution operators and refining themselves via extra mechanisms or modules.
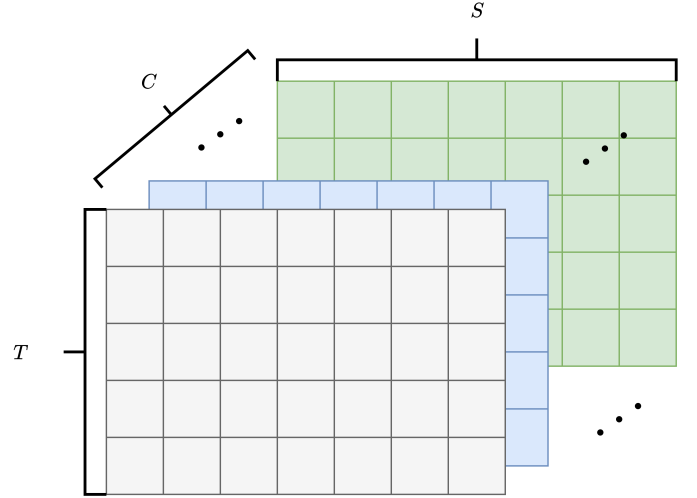

Fig. 1. Input sequence schematic. As long as all variables are spatio-temporal and have an equivalent structure for both dimensions, these sequences can be easily introduced as $C \times T \times S$ images, with variable, temporal and spatial dimension respectively.

III. METHODS

Through this section, we present all the theoretical methods and foundations in which our study bases its ideas and experiments on the role of spatial agnosticism in spatio-temporal series. The code for this paper is available in *https://github.com/rdemedrano/SANN*.

A. Preliminaries

As we intend to demonstrate how the typical intrinsic spatial information given to different forms of convolutional methods is not as important as always assumed, we focus this paper in comparing traditional models with their respective agnostic version. Before explaining this methodologies, we introduce some general aspects.

Given a spatio-temporal sequence X, let us call N to the total number of timesteps and S the total number of spatial points. With this notation, a spatio-temporal sample from the series writes as $x_{t_i,s_j} : i = 1, ..., T; j = 1, ..., S$, being T the total number of timesteps conforming the sample. X_t is the slice of series X for timestep t at all locations, and $X_{T,j}$ is the slice of series X in location j for all timesteps. The predicted series is represented by $\tilde{x}_{t_{i'},s_j} : i = 1, ..., T'; j = 1, ..., S$, where T' is the total number of predicted timesteps. We assume that the number of spatial locations is always the same for both the input and output series.

For all models, the input sequence scheme relies upon a $C \times T \times S$ images as shown in Figure 1, where the number of channels C represents the number of input spatio-temporal variables. During this paper, we will work with $C = 1$ (the studied series by itself), but is easily extensible to any value. Also, all models will consist in one convolution layer outputting a $T \times S \times H$ tensor, where H is the dimension of the new hidden state or number of new channels. This approach allows us to standardize the input and output format of the convolution layers for all methods.
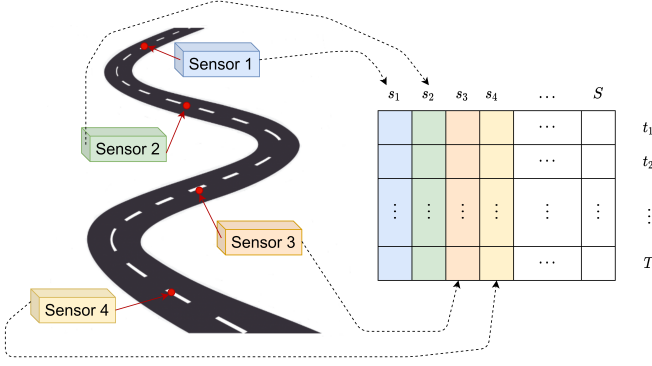
Fig. 2. Example of input tensor definition. Given a network of traffic sensors and its historical series, the objective is predicting future timesteps for all locations using CNNs. The input sequence order in the spatial dimension is usually defined by a logical arrangement of the relative position of the sensors in the network. Traditionally, it is expected to improve network learning through this strategy, generating softer filters by exploiting adjacency relationships.

B. Traditional Convolutional Networks

Now we present the traditional format of convolution-based networks for spatio-temporal series, and we detail how they will be used for testing our main hypothesis.

1) Convolutional Neural Networks (CNN): Convolutional Neural Networks are based on the idea of the convolution operation. Convolution itself ($*$ operator) has the following form for 2D images:

$$(x * K)(i,j) = \sum_{m}^{k_1} \sum_{n}^{k_2} x(m,n)K(i-m,j-n) \quad (1)$$

where K is the kernel. Thus, CNNs are characterized by learning a series of filters which values depend on how adjacent elements are related.

In its classical form, CNNs for spatio-temporal regression rely on ordering the input sequence by spatial adjacency or closeness. Thus, for each row of Fig. 1, spatial zones are mapped into the input tensor in such a way that closer locations are closer in the sequence. By doing so, we make sure that the learnable kernels can take advantage of this *prior* spatial information. The strategies that can be used to adapt convolutional networks to spatio-temporal problems by exploiting this spatial bias based on proximity are multiple (see Section II-B). In our case, the input to the network will be defined as shown in Fig. 2. Similarly, in the temporal dimension (columns) the kernel gathers adjacent timesteps.

2) ConvLSTM Neural Networks: Long Short-Term Memory (LSTM) is a type of recurrent neural network architecture usually used when handling time series data with temporal auto-correlations. A LSTM Neural Network consists of an input gate, an output gate, a memory cell and a forget gate. During the training phase, a weighted function is learned in each of the gates in order to control how much the network "memorize" and "forget".

Based on this model, the ConvLSTM model is a variation of LSTM capable of handling spatio-temporal processes. Comparing with the original LSTM model, the input-to-state

and state-to-state transitions of the ConvLSTM cell involves convolutional operations, making it a well fit for spatial relations. This model is governed by the following equations.

$$
\begin{aligned}
i_t &= \sigma(W_{xi} * X_t + W_{hi} * H_{t-1} + b_i) \\
f_t &= \sigma(W_{xf} * X_t + W_{hf} * H_{t-1} + b_f) \\
C_t &= f_t \circ C_{t-1} + tanh(W_{xc} * X_t + W_{hc} * H_{t-1} + b_c) \quad (2) \\
o_t &= \sigma(W_{xo} * X_t + W_{ho} * H_{t-1} + b_o) \\
H_t &= o_t \circ tanh(C_t)
\end{aligned}
$$

As previously $*$ denotes the convolution operation while $\circ$ denotes the Hadamard product. Furthermore, for timestep t we find that i_t, f_t, o_t are the outputs of input gate, forget gate, and output gate respectively, C_t is the cell output and H_t is the hidden state of a cell.

As explained with CNNs (III-B1), ConvLSTM input sequence is usually ordered by closeness or adjacency in order to take advantage of the shared-weight scheme of the convolution. Through this work, ConvLSTM will use the same input scheme as CNNs as presented in Fig. 2. Thus, convolution operations can make use of this type of spatial relationship.

3) Graph Convolutional Neural Networks (GCN-LSTM): While several proposals have been made during the last years to convolute over graphs, we focus in a particular type presented in [17] called High-Order and Adaptive Graph Convolution, as it has shown good performance in a wide variety of problems. In words of the authors, given a graph $\mathcal{G}$, the k-hop (k-th order) neighborhood is defined as: $N_j = \{v_i \in V | d(v_i, v_j) \leq k\}$ for node v_j. In fact, the exact k-hop connectivity can be obtained by the multiplication of the adjacency matrix A, giving as a result A^k. The convolution is defines as:

$$\tilde{L}_{gconv,t}^{(K)} = (W_k \circ \tilde{A}^k)X_t + B_k, \quad (3)$$

where $\circ$ refer to element-wise matrix product, B is the bias and W a learnable matrix of weights. $\tilde{A}^k$ is defined as $min\{A^k + I, 1\}$.

In order to adapt this kind of networks to spatio-temporal environments, a LSTM layer is stacked with the convolutional one as with ConvLSTM in Section III-B2.

Note that we use nodes to represent the spatial measurement locations, which typically will be sensor stations or road segments, and edges to represent the spatial segments connecting those sensing locations. The adjacency matrix A which defines these spatial segments is usually built based on spatial metrics. For convenience and homogenization, we define for each dataset A as:

$$A_{i,j} = \begin{cases} 1 & (i,j \text{ are neighbors}) \\ 0 & (\text{otherwise}) \end{cases} \quad (4)$$

Where two locations i and j are considered neighbors if they are among the 4 closest areas without counting themselves. Through this definition of A, it is trivial to see that the convolution over each space zone makes use of information based on proximity.
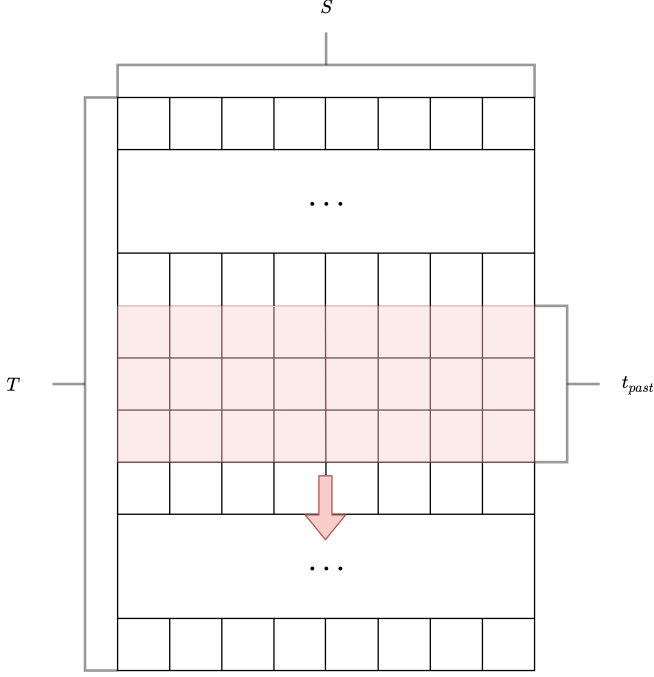
Fig. 3. Example of causal convolution spatially agnostic with $t_{past} = 3$ through a spatio-temporal sequence of just one variable as defined previously.

C. Spatial agnosticism via Convolutional Networks

Now we show a series of spatial agnostic versions based on the models presented through Section III-B for spatio-temporal regression. These methods will help us to test the main hypothesis of this work: whether introducing spatial-adjacency bias is unquestionably the best option or not. For this purpose, each agnostic version needs to fulfill two requirements:

- No spatial information is introduced to the network.
- Past temporal information can be handled and introduced in the calculation of each new state.

By doing so, we will have several spatio-temporal methodologies that let us contrast our main premise.

1) Agnostic Convolutional Neural Network (A-CNN): To define an agnostic version of CNNs, we can work from Equation 1. However, the kernel size is regularly used with equivalent values for its two dimensions $k_1 = k_2 = k$. In this case, not only this kernel uses different values for each component, but kernel size for spatial dimension must be equal to the number of spatial zones: $k_2 = S$. As a result, the convolution operation is made over all locations at once. The kernel size in the temporal dimension is defined as t_{past} and needs to be stipulated as part of the network architecture. An example of this kind of filter can be found in Figure 3.

The temporal dimension is dominated by a causal convolution. Generally, causal convolution ensures that the state created at time t derives only from inputs from time t to $t - t_{past}$. In other words, it shifts the filter in the right temporal direction. Thus t_{past} can be interpreted as how many lags are been considered when processing an specific timestep. Given that previous temporal states are taken into account for each step and that parameters are shared all over the convolution, this methodology might be seen as some kind of memory
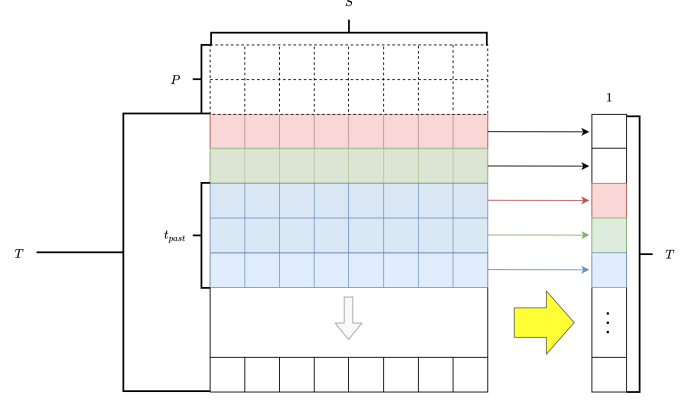

Fig. 4. Illustration of several step of the convolutional part of an agnostic convolutional block. After moving all over the input sequence, a $T \times 1$ image is produced. This new image compress information from all spatial locations and all input lags, keeping track of several of these ones in each convolution.
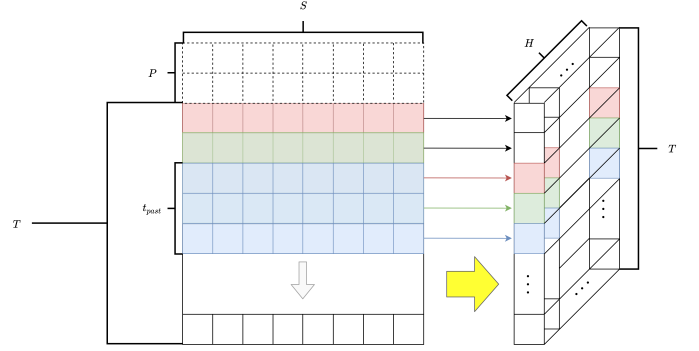

Fig. 5. By repeating operations described before, it is trivial to assemble hidden states as new channels in the latent sequence, meaning $T \times 1$ images with H channels.

mechanism by itself. Unlike memory-based RNNs (like LSTMs and GRUs) where the memory mechanism is integrated solely by learned via the hidden state, in this case t_{past} act as a variable that lets us take some control over this property.

In order to ensure that each input timestep has a corresponding new state when convolving, a padding of $P = t_{past} - 1$ at the top of the input "image" is required, and to guarantee temporal integrity, this padding must be done only at the top. By using convolution in this form, once the kernel has moved over the entire input image $T \times S$, the output image will be $T \times 1$. This process is summarised in Fig 4.

Now, if we repeat this operation H times, we will create a new hidden state with H channels an output an image with $H \times T$ dimensions as the example in Fig 5.

To give the network the opportunity to cover a spectrum of possibilities in terms of expressiveness as wide as a usual CNN for each channel, we simply use transposed convolution with a kernel size $k = (1, S)$ so the system can learn a $T \times S$ representation from a $T \times 1$ image. Fig 6 illustrate this idea.

Evidently, our new representation is usually composed by H hidden states, so this transposed convolution will use H filters. Finally, the complete procedure for an entire agnostic convolutional block is described graphically in Fig 7.

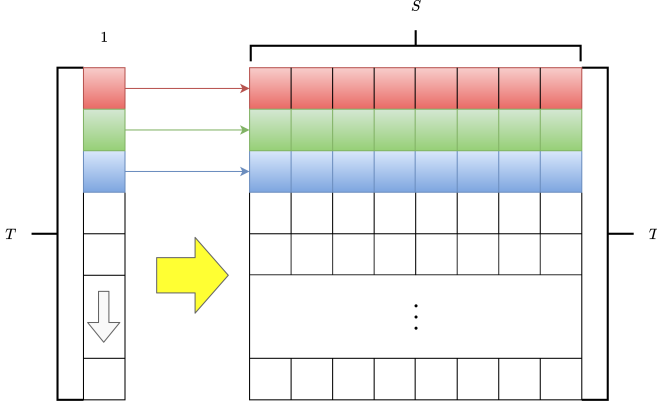Obviously, there are no restrictions with respect to the width

Fig. 6. Transposed convolution to produce a $T \times S$ images from $T \times 1$ latent sequences. Thanks to this process, we give the model same expressiveness opportunities than traditional CNNs.

dimension. For simplicity, we have considered convolutions in which only the number of channels is changed, meaning that images keep an $T \times S$ structure during all the computations. As we have described previously, this will help to normalize our experiments. However, as with CNNs, the dimensionality of hidden and output states might be different. Over all this process, the arrangement of the spatial dimension (columns) has no effect, meaning that it is not it is not necessary to map the study areas in any specific way with the input of the network, as was done with the CNNs (Fig. 2).

2) Agnostic ConvLSTM (A-ConvLSTM): Once that the agnostic procedure for convolving has been presented in the previous section, the A-ConvLSTM is governed by Equation 2 but changing the traditional convolution for this new approach. The only difference with respect to A-CNN is that there is no need of causal convolution over the temporal dimension, as the LSTM module can handle it. Therefore, the input sequence lacks any spatial ordering procedure, letting us define this dimension arbitrarily.

3) Agnostic Graph Convolutional Network (A-GCN-LSTM): Following the structure of the GCN-LSTM presented in Section III-B3, its agnostic version is simply to define the adjacency matrix as the identity matrix: $A = I_S$. Thus, we can make sure that no spatial relation is being introduced or modeled explicitly. Otherwise, the network has the same functioning and characteristics as described before.

A comparison between each traditional model and its agnostic version is shown in Table I. There it is summarized how each model formalize *prior* information about the spatial dimension and how it affects their use.

D. Regressor block

Through Sections III-B and III-C, we have explored how to use convolution operations to learn a new hidden representation of the input sequence as an image with and without using *prior* spatial information or closeness assumptions. Now, in order to make a fair comparison between traditional networks and their respective agnostic versions, we have to carefully use this latent representation with $T \times S \times H$ dimensions (common to all models presented) to get a new $T' \times S$ predicted image.

TABLE I
SUMMARY OF SPATIAL TREATMENT OF EACH MODEL.

	Traditional	Agnostic
CNN	Shared kernel among locations. Ordering of spatial dimension based on closeness	One kernel for each location. No ordering needed
ConvLSTM	Shared kernel among locations. Ordering of spatial dimension based on closeness	One kernel for each location. No ordering needed
GCN-LSTM	Adjacency matrix defined by proximity	Identity matrix as adjacency matrix

While this process can be done in multiple ways, it is desirable for this regressor block to fulfill several conditions:

(1) The same strategy has to be applicable to all models studied in this work.
(2) It can not explicitly share information between elements of the spatial dimension. This way, we make sure that space is only treated in the convolutional block of each model and our results are not contaminated from other parts of the network.
(3) The number of parameters needs to be as low as possible and space-independent. Thus, we avoid overfitting or overinfluence problems.
(4) Lastly, although we have not found an option that is completely network architecture-independent (you can get a similar size of hidden dimension or total number of parameters, but not both), it is highly desirable that this regressor layer does not undergo too much variability between models.

A naive and simple approach would be using 1D convolutions after reshaping the $H \times T \times S$ image into a $(H \cdot T) \times S$, with $H \cdot T$ being the number of input channels. By convolving trough the spatial dimension with a kernel size of $k = 1$ and an output number of channels of T', we can be sure no information is shared through this dimension (2) and the number of parameters, which is $H \cdot T \cdot T'$, remains low compared to the complete network (3). Furthermore, all models that we will compare are based on a convolutional block which outputs an $H \times T \times S$, meaning that this regressor scheme can be applied to all of them, helping to standardize our experiments (1). As T is the same for all models and H never diverges more than one order of magnitude, we can be sure this layer has a similar impact for all cases (4). Fig 8 summarize this block.

Although other options have been considered, as 2D convolutions and dense layers, they fail to meet some conditions or need fine-tuning for each problem and model, making them less suitable for a fair comparison.

E. Temporal vs spatial distribution

Our work is based on the hypothesis that real spatio-temporal series might not share a similar behavior in their two dimensions. Even the well known fact that closer, spatially speaking, locations behaves similarly does not always suit well, meaning that the parameter sharing scheme of traditional CNNs might not be the best option. Concretely, when dealing with real
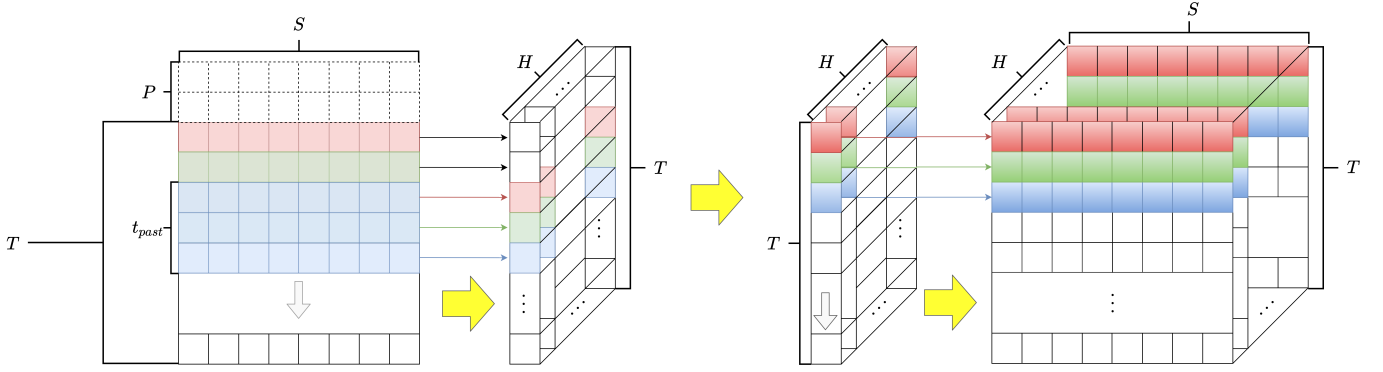
Fig. 7. Representation of a complete agnostic convolutional block. By assembling operations described before, from a $T \times S$ it is trivial to create hidden states capable of representing equivalent expressions compared to a traditional CNN, meaning $T \times S$ images with H channels.
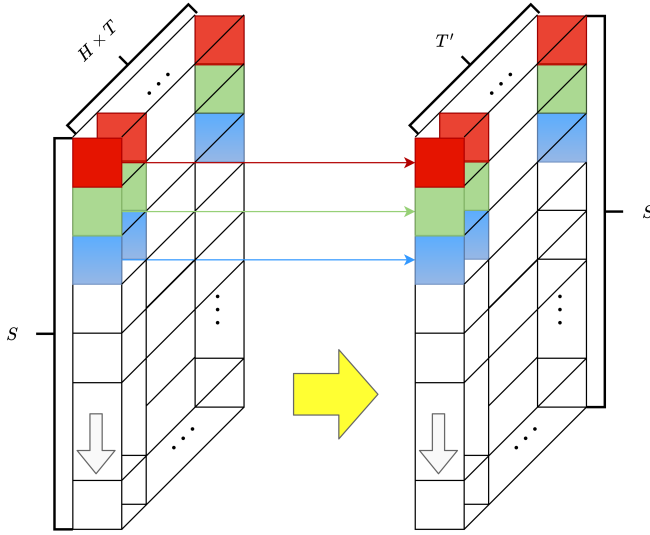

Fig. 8. Regressor block that satisfy applicability, spatial agnosticism and simplicity. By using a 1D convolution over the latent image $H \times T \times S$, we can produce a $T' \times S$ sequence that correspond to our forecast.

problems, the system might have a high dependency on non-spatial phenomena and data collection can have a great impact. As a result, closeness information can be lost or modified.

On the contrary, temporal information (or distribution) usually keeps the same structure for a wide range of problems. As air quality and mobility are high correlated to human being, the temporal pattern of this kind of series for each location tends to remain alike.

In order to prove our hypotheses, we will make use of statistical tools that characterize the aforementioned information.

1) Spatial dimension: Moran's I: According to [25], "Spatial autocorrelation or spatial dependence can be defined as a particular relationship between the spatial proximity among observational units and the numeric similarity among their values; positive spatial autocorrelation refers to situations in which the nearer the observational units, the more similar their values (and vice versa for its negative counterpart)... This feature violates the assumption of independent observations upon which many standard statistical treatments are predicated." This property, which is precisely what we are interested in,

can be measured by the well know Moran's I. This test will let us quantify the degree of spatial autocorrelation existing in the different datasets that we will use between close locations taking into account this interdependency. As it is a test, Moran's I comes with a p-value which typifies statistical significance of the result. It is defined as:

$$I = \frac{S}{W} \frac{\sum_i \sum_j w_{ij}(x_i - \bar{x})(x_j - \hat{x})}{\sum_i (x_i - \bar{x})^2} \quad (5)$$

where S is the number of spatial units indexed by i and j, x is the variable of interest, $\bar{x}$ is the mean of x, w_{ij} is a matrix of spatial weights based on neighbors, and W is the sum of all w_{ij}. As its value varies usually between -1 and $+1$, it is easily interpretable. Concretely, $+1$ implies similar values for close locations, 0 a random arrangement, and -1 opposite values.

As we also have a temporal dimension, we will average I for all timesteps. Through this test we want to compute solely spatial autocorrelation, without intervention of temporal relations between locations.

2) Temporal dimension: Adaptive Temporal Dissimilarity Measure: To compare the similarity between different time series (in our case, different spatial points) the same problem arises than with spatial autocorrelation: due to the interdependence relationship between measurements classical correlation index can not be applied. For example, Euclidean, Fréchet distances and Dynamic time warping are well known and widely used techniques when measuring time series similarity but do not handle the aforementioned issue well. To solve this problem, [26] proposed the Adaptive Temporal Dissimilarity Measure (ATDM) as an index that lets us measure the similarity between time series more robustly as it balances the proximity with respect to values and the proximity with respect to behavior. Ir writes as:

$$\begin{aligned} \text{ATDM}(X_{T,i}, X_{T,j}) = \\ f(\text{cort}(X_{t,i}, X_{t,j})) \cdot \delta(X_{t,i}, X_{t,j}), \end{aligned} \quad (6)$$

where δ references a classical distance (we will use Eu-

clidean) and cort is

$$\text{cort}(X_{T,i}, X_{T,j}) =$$
$$\frac{\sum_t^{T-1}(X_{t+1,i} - X_{t,i})(X_{t+1,j} - X_{t,j})}{\sqrt{\sum_t^{T-1}(X_{t+1,i} - X_{t,i})^2}\sqrt{\sum_t^{T-1}(X_{t+1,j} - X_{t,j})^2}}. \quad (7)$$

Lastly, f writes as follow:

$$f(x) = \frac{2}{1 + \exp(kx)}, k \geq 0. \quad (8)$$

With this metric, the distance is squeezed into a coefficient in the interval $(0, 2)$. When the correlation coefficient is 0, the ATDM is 1, and the correlation is not significant. When the correlation is positive, the value of the ATDM is less than 1; the more similar the two series are, the smaller the value is. On the contrary, the ATDM is more than 1 if the correlation is negative. The less similar the two series are, the larger the value is.

Thus, we can average the ATDM between all locations pairs for each spatio-temporal series. As this measure takes into account both values and behavior of the series, we can approximately get a global measure of temporal distribution similarity among points for each dataset.

When working with real data, in which depending on time granularity local properties of time series might be noisy, ATDM might not extract information correctly. In order to solve this, we compute an adjusted ATDM coefficient (ATDM_{adj}) which uses a smoother version of the input series as we are interested in global behavior of the temporal distribution. Concretely, we use moving average as it is simple and has shown to be a good approximator for time series. As moving average just smooth the series, we do not expect to corrupt the coefficient between series which are not really temporally correlated.

IV. EXPERIMENTAL DESIGN

A. Data description

The different forecasting problems and the corresponding datasets are described below. Main dataset characteristics and statistics are provided in Table II.

- **AcPol dataset:** Provided by the Municipality of Madrid through its open data portal[1]. Acoustic pollution in Madrid in decibels, it measures equivalent continuous level with A frequency weighting, which is the assumed noise level constant and continuous over a period of time, corresponding to the same amount of energy than that actual variable level measured in the same period.
- **Beijing dataset:** Presented by [27], it consist of traffic speed measurements for 15000 road segments recorded per minute. To make the traffic speed predictable for each road segment, it is aggregated via moving average in 15 minutes intervals. For this work, we select a subgroup of road segments spatially close.

- **BiciMad dataset:** Supplied by EMT (Municipal Transport Company for its initials in Spanish) through its open data portal[2]. In this case we tackle the bike sharing demand prediction by aggregating the overall number of bikes per station and timestep.
- **LOOP dataset:** It contains data collected from inductive traffic loop detectors deployed on four connected freeways (I-5, I-405, I-90, and SR-520) in the Greater Seattle Area. It can be found in [28].
- **MATRA dataset:** This dataset contains historical data of traffic measurements in the city of Madrid. The measurements are taken every 15 minutes at each point, including traffic intensity in number of cars per hour. Data is aggregated for each hour. While a dense and populated network of over 4.000 sensors is available, we decided to simplify and use only a selection of them. Available in the Municipality of Madrid open data portal[1].
- **METR-LA dataset:** This dataset contains traffic information recopilated from loop detectors in the highway of Los Angeles County. We use the partition provided by [14].
- **NO2 dataset:** NO_2 in the city of Madrid. Hourly data for all measurement stations which include this pollutant. Available in the Municipality of Madrid open data portal[1].
- **NYTaxi dataset:** Provided by Taxi & Limousine Commission [3], it consist of taxi trip location and duration in the city of New York. We focus our work in forecasting number of taxi travels for each New York neighborhood with an average minimum number of one trip per day.
- **O3 dataset:** O_3 in the city of Madrid. Hourly data for all measurement stations which include this pollutant. Available in the Municipality of Madrid open data portal[1].
- **PEMS-BAY dataset:** This traffic dataset is collected by California Transportation Agencies (CalTrans) Performance Measurement System (PeMS). We use the partition provided by [14].

All datasets are Z-Score normalized by spatial point. We take as reference previous work as a criterion to choose T and T'. Thus, we can be sure of the plausibility of the results for all models. When no previous work is known, we use autocorrelation as a measurement of number of minimum lags (T) and focus only on a single timestep prediction ($T' = 1$).

From Table II we can see how our chosen datasets cover a wide range of spatio-temporal circumstances and the high variety and variability of data. Also, our main hypotheses are confirmed: Moran's I show a clear no-spatial autocorrelation pattern for our series, and although not completely uncorrelated, most series are close to 0. All p-values are lower than 0.05. It is worth noting as proof of plausibility for these values that [18] computed the coefficient I for the complete Beijing traffic dataset at some hours, reporting a similar value to ours. ATDM values tend to be low, which is representative of similar temporal distributions in the datasets. As we expected, ATDM_{adj} represents better this idea. Datasets with a clear

---

temporal pattern but locally noisy, as Beijing, LOOP, and PEMS-BAY, are better described by this coefficient.

Given that spatial locations are by default in arbitrary order, it is necessary to sort and structure them in order to fully exploit spatial information with traditional models. By computing a hierarchical tree (dendrogram) using an agglomerative hierarchical clustering algorithm and traversing recursively the tree it is possible to approximately sort the points by distance.

B. Architecture models

We compare agnostic models with widely used spatio-temporal series regression models based on the convolution operator. Details concerning its architectures are:

- **A-CNN:** Through the process batch normalization and ReLU activation function are used.
- **CNN:** A standard CNN followed by a batch normalization layer and ReLU activation function. It uses a 3×3 kernel.
- **A-ConvLSTM:** ReLU activation function after convolution. No batch normalization.
- **ConvLSTM:** A standard ConvLSTM that uses a 3×3 kernel. ReLU activation function after convolution. No batch normalization.
- **A-GCN-LSTM:** ReLU activation function.
- **GCN-LSTM:** A classical approach for GCN which let us exploit explicitly information from the k-hop (k-th order) neighborhood of each node in the graph. In our experiments, we set $k = 3$ and use ReLU activation function.

As we are interested in deepening in how the convolution operator and the spatial dimension are related, we do not include any RNN or FNN based approach.

C. Experimental design

In order to make a comparison as fair as possible, we decided to proceed with all models as follows:

- They will consist uniquely in a convolutional layer and a regressor layer. For all of them, the convolutional layer will enrich input information by constructing a $H \times T \times S$ image from a $T \times S$ sequence as described in Section III-A.
- The regressor layer consists of a 1D convolution, as explained in Section III-D. Thus, we make sure no model is taking advantage or exploiting further spatial information.
- The number of parameters in the convolutional layer need to remain similar and in the same magnitude order. Given regressor layer's architecture and the fact that it is the same for all models, we expect that this is enough to eliminate possible bias.
- A weight decay (L2 regularization) of 10^{-3} is used to prevent overfitting.

Some other minor details are that all the models are trained using the mean squared error (MSE) as objective function with the RMSprop optimizer, as it has shown good performance in non-stationary scenarios. Batch size is 256, momentum is set to 0.9, the initial learning rate is 0.001 and both early stopping and learning rate decay are implemented in order to avoid overfitting and improve performance. The experiments are run in a NVIDIA RTX 2070.

As we have standardized the experiments, no hyperparameter tuning is needed in general. Solely t_{past} for A-CNN needs to be adjusted, which will be tuned via standard grid search.

D. Validation and error metrics

As stated in [29], standard k-cross-validation is the way to go when validating neural networks for time series if several conditions are met. Specifically, that we are modeling a stationary nonlinear process, that we can ensure that the leave-one-out estimation is a consistent estimator for our predictions and that we have serially uncorrelated errors.

While the first and the third conditions are trivially fulfilled for our problem, the second one needs to be specifically treated. Given that some input sequences might share elements among different sets(training, validation and test), *prior* information could be entangled leading to data leakage. Due to this problem, it is not possible to create random folds and it is necessary to specify a separation border among previously defined sets. Particularly, a 10-cross-validation scheme without repetition is used during all experiments, with a 80%/10%/10% scheme for train/validation/ test sets for each fold.

To evaluate the precision of each model, we computed root mean squared error (RMSE) and bias. In a spatio-temporal context [30], they are defined as:

$$\text{RMSE} = \sqrt{\frac{1}{T'S} \sum_{i=1}^{T'} \sum_{i=1}^{S} (\tilde{x}_{t'_i,s_j} - x_{t'_i,s_j})^2}, \qquad (9)$$

$$\text{bias} = \frac{1}{T'S} \sum_{i=1}^{T'} \sum_{j=1}^{S} (\tilde{x}_{t'_i,s_j} - x_{t'_i,s_j}), \qquad (10)$$

For all these metrics, the closer to zero they are the better the performance is. While RMSE already provides a dispersion measure respect to real series, bias is better to find particular predispositions when making predictions.

V. RESULTS

A. Performance comparison

A general comparison of the different error metrics can be seen in Table III.

First of all, we can verify the goodness of our experiments by direct comparison with analogous studies [13], [14], [27], [28], [31], showing that our results are in line with them. Since most of the datasets have already been used, we can extrapolate this idea to those which have not. To better visualize the error over all datasets, Fig. 9 shows RMSE distribution. From this figure we can deduct that, in general terms, agnostic models show a similar behavior than their respective main competitors.

The performance of the different strategies over individual datasets is directly associated with the spatial autocorrelation metric in Table II. On the one hand, datasets with a higher value of Moran's I have a propensity to show better performance

TABLE II
DETAILS OF DATA THROUGH EXPERIMENTS. $Dates$ REFLECTS STARTING AND ENDING POINTS OF DATA, $Timestep$ CORRESPONDS TO THE DURATION OF ONE TIMESTEP. T, T' AND S WERE DEFINED IN SECTION III-A AS INPUT TIMESTEPS, OUTPUT TIMESTEPS AND NUMBER OF SPATIAL LOCATIONS. $Mean$, $Median$, AND Std CONDENSE MAIN DATA STATISTICS. $ATDM$, $ATDM_{adj}$, AND $Moran's\ I$ SUMMARIZE INFORMATION ABOUT SPATIAL AND TEMPORAL DISTRIBUTION SIMILARITY BETWEEN LOCATIONS.

Dataset	Dates	Timestep	T	T'	S	Mean	Median	Std	ATDM	ATDM$_{adj}$	Moran's I
AcPol	2014/01/01 – 2019/03/31	1 day	7	1	30	56.8	60.2	15.1	0.36	0.36	0.03
Beijing	2017/01/04 – 2017/05/31	15 min	10	1	200	29.0	28.7	9.3	0.69	0.27	0.20
BiciMad	2019/01/01 – 2019/06/30	1 hour	6	1	168	0	0	3.2	1.04	1.03	0.12
LOOP	2015/01/01 – 2015/03/31	5 min	10	1	323	57.2	60.6	11.8	0.84	0.47	0.31
MATR	2018/01/01 – 2019/12/31	1 hour	24	6	120	445.5	254.8	539.6	5.6E-4	4.8E-4	0.09
METR-LA	2012/03/01 – 2012/06/30	5 min	12	3	207	53.4	62.3	20.6	0.02	0.02	0.24
NO2	2017/01/01 – 2019/12/31	1 hour	48	48	24	37.5	29	28.9	0.04	0.0	0.13
NYTaxi	2016/01/01 – 2016/06/30	1 hour	6	1	70	4.8	0	11.3	0.55	0.34	0.24
O3	2017/01/01 – 2019/12/31	1 hour	48	48	14	50.6	50	34.3	0.03	0.0	0.11
PEMS-BAY	2017/01/01 – 2017/05/31	5 min	12	3	325	62.6	65.3	9.6	0.64	0.15	0.23

TABLE III
AVERAGE PERFORMANCE PER MODEL AND DATASET. FOR A MORE DETAILED VIEW OF ERROR METRICS DISTRIBUTION, SEE FIG. 9.

	AcPol		Beijing		BiciMad		LOOP		MATR	
	RMSE	Bias	RMSE	Bias	RMSE	Bias	RMSE	Bias	RMSE	Bias
A-CNN	7.06	0.22	2.74	0.02	2.75	-2.0E-4	5.06	-0.07	115.65	-5.30
CNN	8.52	-0.04	4.52	-0.02	2.94	-0.01	4.59	0.05	141.99	0.13
A-ConvLSTM	6.22	0.04	2.64	7.3E-3	2.74	-8.3E-3	4.52	0.02	111.74	-0.06
ConvLSTM	5.46	-3.0E-3	2.26	-0.15	2.89	-0.01	3.71	0.03	115.29	-2.85
A-GCN-LSTM	7.45	0.17	2.88	0.02	2.76	6.7E-4	5.77	-0.53	136.48	2.97
GCN-LSTM	8.01	0.03	2.76	0.09	2.70	6.2E-3	5.02	-0.18	132.14	0.43

	METR-LA		NO2		NYTaxi		O3		PEMS-BAY	
	RMSE	Bias	RMSE	Bias	RMSE	Bias	RMSE	Bias	RMSE	Bias
A-CNN	9.52	0.29	23.17	0.27	2.97	0.02	22.13	1.51	3.98	-0.03
CNN	10.00	-0.01	24.26	-0.03	3.52	0.06	23.30	0.607	3.98	0.03
A-ConvLSTM	9.13	0.24	22.79	0.01	2.86	1.3E-4	21.56	1.00	3.66	-0.03
ConvLSTM	7.86	-0.05	24.25	0.31	3.16	-0.01	21.56	0.71	2.42	0.04
A-GCN-LSTM	10.14	0.14	23.51	0.23	2.87	2.7E-3	22.71	0.25	4.16	0.14
GCN-LSTM	10.17	-0.58	24.98	-0.90	2.88	0.01	23.39	1.75	4.07	-0.68

with traditional models (Beijing, Loop, METR-LA, and PEMS-BAY). On the other hand, datasets with lower values of the same metric usually show better behavior with the agnostics versions (AcPol, BiciMad, MATR, NO2, NYTaxi, and O3).

In order to inquire into these results and provide statistical evidence, a Friedman rank test was performed over the error distribution for all datasets. A Friedman statistic of $F = 21.6$, distributed according to a χ^2 with 5 degrees of freedom obtains a p-value of $6.2e-4$ with $\alpha = 0.05$, which provides evidence of the existence of a significant difference between the algorithm.

Given that Friedman's null hypothesis was rejected, a post-hoc pairwise non-parametric based comparison was carried out to check the differences between the proposed algorithms with Holm and Benjamini-Hochberg adjustments. As we are especially interested in testing whether the introduction of spatial information as a *prior* is necessary or not, Table IV shows statistical significance in the traditional-agnostic model comparison for all datasets. Through these tests we compare if there are significant differences between the means of two different algorithms error distributions. Thus, for each hypothesis the test accepts or rejects the idea that the two models that compose the hypothesis generate, statistically speaking, same error distributions. By looking at this table we

TABLE IV
ADJUSTED HOLM AND BENJAMINI-HOCHBERG p-VALUES WITH PAIRWISE REJECTED HYPOTHESIS AT $\alpha = 0.05$ FOR ALL DATASETS. A p-VALUE LOWER THAN α SUGGEST THAT BOTH ALGORITHMS PRODUCE DIFFERENT ERROR DISTRIBUTIONS.

i	hypotheses	$p_{\text{unajusted}}$	p_{holm}	p_{BH}
I	A-CNN vs CNN	0.014	0.048	0.023
II	A-ConvLSTM vs ConvLSTM	0.77	1	0.825
III	A-GCN-LSTM vs GCN-LSTM	0.736	1	0.846

can confirm our initial claim since there is not enough evidence to support that traditional methods suppose an improvement over their agnostic versions. In fact, the only comparison that yields a significant result (hypothesis I) show evidence in favor of the agnostic model.

In terms of computational performance, Table V summarises average run times per fold, model, and dataset, and the number of parameters per dataset for all models (recall that, to facilitate a fairer comparison, all models have the same number of parameters for every problem, see Section IV-C). Again, no differences are reported between traditional and agnostic models neither. As we would expect, A-CNN and CNN models show great advantage in terms of time consumption compared to the rest of the methodologies.
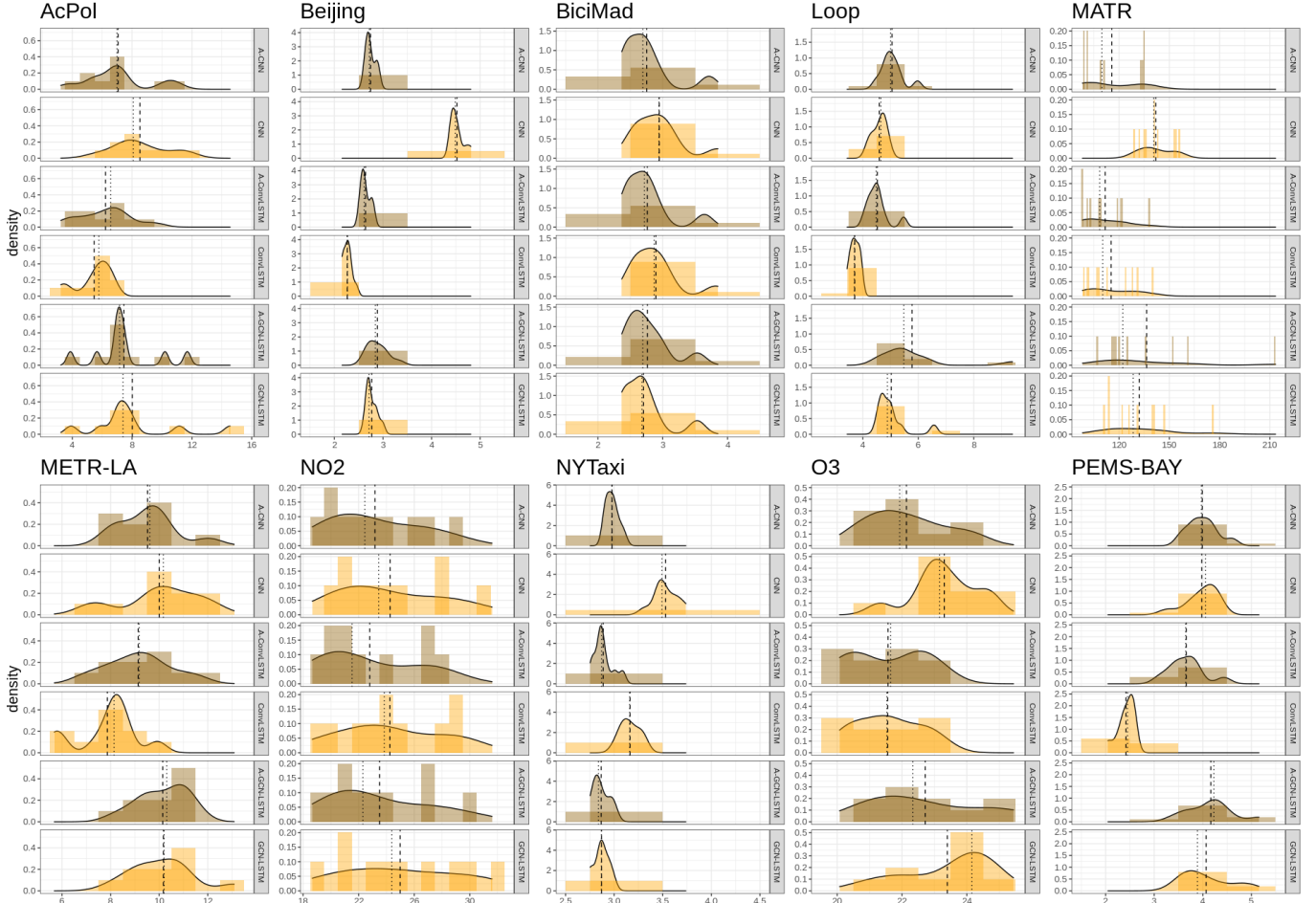
RMSE

Fig. 9. RMSE distribution for each model and dataset. Dashed vertical line represents the mean, dotted vertical line represents median.

TABLE V
AVERAGE RUN TIME PER FOLD IN SECODS AND APPROXIMATE NUMBER OF PARAMETERS USED PER DATASET.

	AcPol	Beijing	BiciMad	LOOP	MATR	METR-LA	NO2	NYTaxi	O3	PEMS-BAY	Average
A-CNN	1.0	16.7	4.1	97.7	26.7	36.5	56.8	42.8	42.8	67.9	36.3
CNN	1.4	8.1	13.4	117.5	44.5	68.6	33.2	18.4	22.5	48.0	37.8
A-ConvLSTM	4.8	41.9	5.1	229.1	411.8	179.6	67.8	9.2	56.2	349.0	135.5
ConvLSTM	2.6	103.2	38.2	350.0	422.5	238.7	74.8	13.0	56.8	400.7	171.6
A-GCN-LSTM	18.1	72.6	15.0	168.7	146.0	83.7	449.4	24.4	221.2	172.3	137.1
GCN-LSTM	13.3	71.9	12.5	190.5	111.7	77.9	467.4	30.5	221.6	199.9	141.0
Number of parameters	∼ 50K	∼ 200K	∼ 150K	∼ 250K	∼ 200K	∼ 150K	∼ 200K	∼ 150K	∼ 150K	∼ 250K	

B. Spatial agnosticism: permutation test

To further validate one the most important statements of this work, i.e. to ensure that the models we have presented as spatially agnostic really are, we propose to randomly permutate the spatial dimension of data before training. As we just want to compare the behavior of the different methods when input data is not sorted, we are only interested in studying how the error distributions are modified when this perturbation is introduced in the system, and not in pure performance. Given that ConvLSTM and A-ConvLSTM have shown to be a statistically significant better option than the other models, we will use only these two models through this section.

In Fig. 10 we can visualize the RMSE results for both models before and after (*model name-perm*) the random permutation.

From this last figure we can clearly see that error distributions for A-ConvLSTM and A-ConvLSTM-perm are practically identical for all the problems, while that does not happen for ConvLSTM and ConvLSTM-perm. Thus, we carry out a post-hoc pairwise non-parametric based comparison to check the differences between the models with Holm and Benjamini-Hochberg adjustments. Table VI shows the aforementioned p-values, marking with asterisks (*) those that are statistically significant. In the table, "A-ConvLSTM" refers to the comparison A-ConvLSTM vs A-ConvLSTM-perm, while "ConvLSTM" refers to the comparison ConvLSTM vs ConvLSTM-perm.

This table lets us conclude that A-ConvLSTM shows spatial agnosticism and its performance is unaffected by how the spatial dimension is treated. However, the ConvLSTM presents
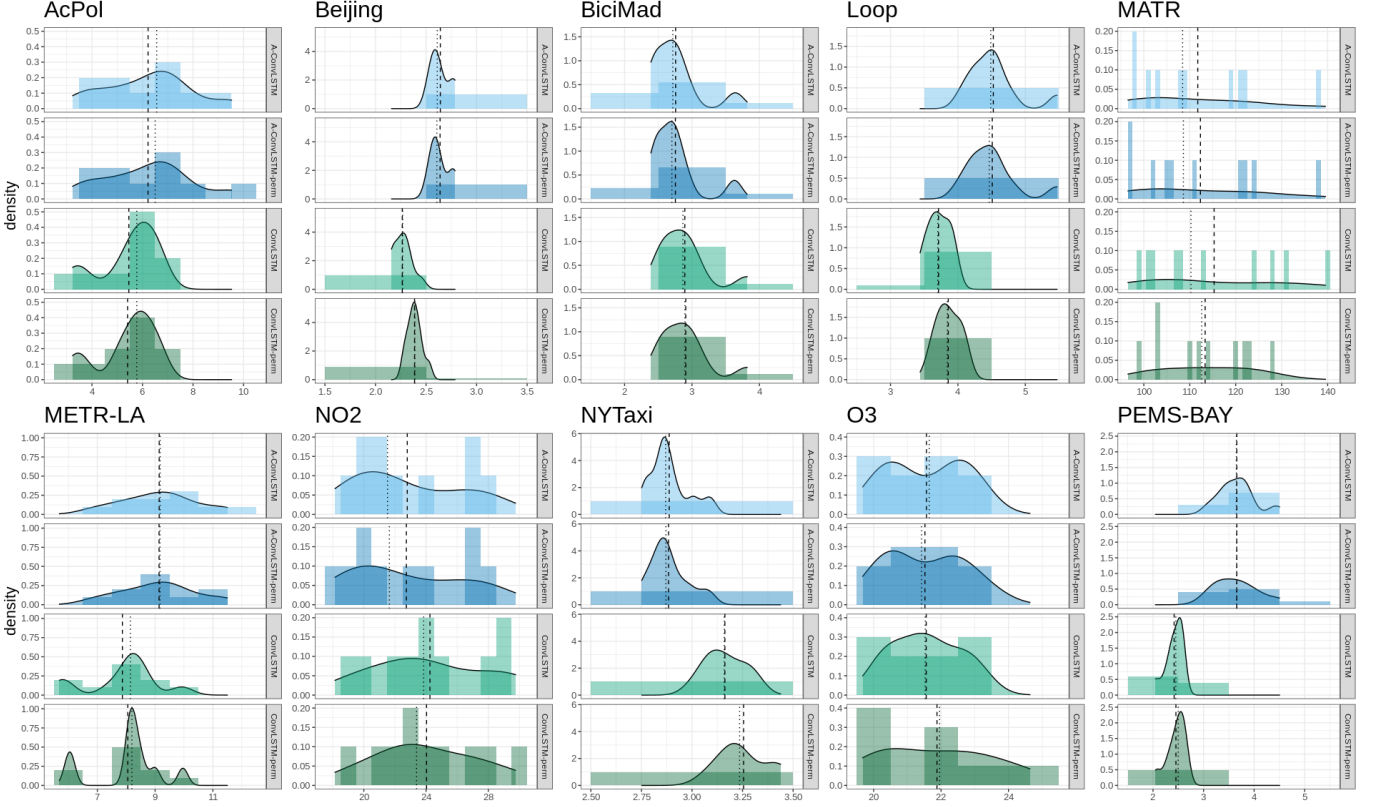
RMSE

Fig. 10. RMSE distribution for each model and dataset before and after training with randomly permutations in their spatial dimension. Dashed vertical line represents the mean, dotted vertical line represents median. In blue, A-ConvLSTM-based models and in green ConvLSTM-based models.

TABLE VI
ADJUSTED HOLM AND BENJAMINI-HOCHBERG p-VALUES WITH PAIRWISE REJECTED HYPOTHESIS AT $\alpha = 0.05$ FOR ALL DATASETS AFTER TESTING SPATIAL AGNOSTICISM VIA RANDOM PERMUTATION. REJECTED HYPOTHESIS (MEANING BOTH ALGORITHMS PRODUCE DIFFERENT ERROR DISTRIBUTIONS) ARE MARKED WITH *.

	AcPol			Beijing			BiciMad			LOOP			MATR		
	$p_{unajusted}$	p_{holm}	p_{BH}	$p_{unajusted}$	p_{holm}	p_{BH}	$p_{unajusted}$	p_{holm}	p_{BH}	$p_{unajusted}$	p_{holm}	p_{BH}	$p_{unajusted}$	p_{holm}	p_{BH}
A-ConvLSTM	0.922	1	0.922	0.193	0.193	0.193	0.496	0.496	0.496	0.027*	0.027*	0.027*	0.232	1	0.668
ConvLSTM	0.922	1	0.922	0.014*	0.027*	0.016*	0.027*	0.027*	0.027*	0.002*	0.012*	0.002*	0.557	1	0.668

	METR-LA			NO2			NYTaxi			O3			PEMS-BAY		
	$p_{unajusted}$	p_{holm}	p_{BH}	$p_{unajusted}$	p_{holm}	p_{BH}	$p_{unajusted}$	p_{holm}	p_{BH}	$p_{unajusted}$	p_{holm}	p_{BH}	$p_{unajusted}$	p_{holm}	p_{BH}
A-ConvLSTM	0.777	0.777	0.777	0.777	0.984	0.777	0.375	0.375	0.375	0.557	1	1	0.846	0.846	0.846
ConvLSTM	0.011*	0.02*	0.012*	0.492	0.984	0.59	0.01*	0.022*	0.013*	0.846	1	0.846	0.004*	0.012*	0.005*

an important discrepancy in terms of performance when unsorting the grid. Although this premise holds in general terms over all datasets, it can be seen again that the results are directly related to correlation metrics in Table II: those datasets with a higher value of Moran's I tend to suffer more with the permutation test (Beijing, LOOP, METR-LA, and PEMS-BAY). As in those cases the spatial autocorrelation is higher, sharing parameters in the spatial dimension is more beneficial, and changing the grid has a greater effect.

C. Practical guidelines

Given our results, we can provide some guidelines in order to help other practitioners working with real spatio-temporal problems:

- Assuming neighborhood-based relations as a premise when approaching a spatio-temporal problem with neural networks might not always be the best option. Instead of naively assuming these spatial relations, it might be beneficial to dig more deeply in the data analysis or to rethink how the problem is addressed. Concretely, real datasets do not necessarily are similar through spatial locations, contrary to what is usually assumed. Thus, the nature of data should be reflected when defining the network architecture. In any case, further considerations should be given to preliminaries studies of the spatial distribution of the data.
- When the distribution of the data shows a clear spatial relationship based on neighborhood, as in the case

of large traffic sensor networks, the traditional format of convolution-based networks might be advantageous. However, when this is not clearly verified, as for example with air quality, models do not show improvement by sharing weights between different locations.

- If there is not enough available evidence about the spatial distribution characteristics, spatially agnostic models might be best suited as they are capable of performing well while being less laborious to work with.
- In any case, consider using spatial agnostic models if your needs in terms of precision must be balanced with the available resources.

VI. CONCLUSIONS

Through this work, we have explored how classical spatial assumptions based on closeness are not always the best deal when working with convolutional neural networks for spatio-temporal series regression. Due to their usual lack of spatial autocorrelation, other alternatives might be more suited. In order to test this idea, we have compared several versions of convolutional-based models that make no use of *prior* spatial information (neither directly nor indirectly), namely spatial agnostic, with their respective traditional forms. Spatial agnostic models are a perfect tool to contrast our hypothesis as they do not use extra modules or steps as others, but tackle the problem directly purely via convolutions.

After extensive and standardized experimentation, we can confirm our main hypothesis: the inclusion of adjacency-based representations of the spatial distribution of real data does not necessarily fit well for the classical convolutional shared-weights scheme. Concretely, without using any specific spatial mechanism, spatial agnostic models have been shown to be equal in performance to some of the most notable spatio-temporal models. Also, we have shown how these models, unlike traditional convolutional methods, are really spatially agnostic, and how this is related to the spatial autocorrelation of the series. Furthermore, beyond proving our initial hypothesis we have shown how our methodology is simpler and less laborious to work with, offering the possibility of obtaining good performance without having to carry out extra research about the application domain. Finally, by analyzing ten different datasets with different spatio-temporal conditions each, we can confirm the statistical significance of these statements with a confidence of 95%.

VII. ACKNOWLEDGEMENTS

REFERENCES

[1] Y. LeCun, B. Boser, J. S. Denker, D. Henderson, R. E. Howard, W. Hubbard, and L. D. Jackel, "Backpropagation applied to handwritten zip code recognition," *Neural computation*, vol. 1, no. 4, pp. 541–551, 1989.

[2] A. Krizhevsky, I. Sutskever, and G. E. Hinton, "ImageNet Classification with Deep Convolutional Neural Networks," in *Advances in Neural Information Processing Systems 25*, F. Pereira, C. J. C. Burges, L. Bottou, and K. Q. Weinberger, Eds. Curran Associates, Inc., 2012, pp. 1097–1105. [Online]. Available: http://papers.nips.cc/paper/4824-imagenet-classification-with-deep-convolutional-neural-networks.pdf

[3] Y. Taigman, M. Yang, M. Ranzato, and L. Wolf, "DeepFace: Closing the Gap to Human-Level Performance in Face Verification," in *2014 IEEE Conference on Computer Vision and Pattern Recognition*, Jun. 2014, pp. 1701–1708, iSSN: 1063-6919.

[4] B. Zhao, H. Lu, S. Chen, J. Liu, and D. Wu, "Convolutional neural networks for time series classification," *Journal of Systems Engineering and Electronics*, vol. 28, no. 1, pp. 162–169, Feb. 2017, conference Name: Journal of Systems Engineering and Electronics.

[5] Z. Cui, W. Chen, and Y. Chen, "Multi-Scale Convolutional Neural Networks for Time Series Classification," *arXiv:1603.06995 [cs]*, May 2016, arXiv: 1603.06995. [Online]. Available: http://arxiv.org/abs/1603.06995

[6] F. Rodrigues and F. C. Pereira, "Beyond Expectation: Deep Joint Mean and Quantile Regression for Spatiotemporal Problems," *IEEE Transactions on Neural Networks and Learning Systems*, pp. 1–13, 2020, conference Name: IEEE Transactions on Neural Networks and Learning Systems.

[7] E. Tu, N. Kasabov, and J. Yang, "Mapping Temporal Variables Into the NeuCube for Improved Pattern Recognition, Predictive Modeling, and Understanding of Stream Data," *IEEE Transactions on Neural Networks and Learning Systems*, vol. 28, no. 6, pp. 1305–1317, Jun. 2017, conference Name: IEEE Transactions on Neural Networks and Learning Systems.

[8] H. Nam and B. Han, "Learning Multi-Domain Convolutional Neural Networks for Visual Tracking," 2016, pp. 4293–4302.

[9] A. Kappeler, S. Yoo, Q. Dai, and A. K. Katsaggelos, "Video Super-Resolution With Convolutional Neural Networks," *IEEE Transactions on Computational Imaging*, vol. 2, no. 2, pp. 109–122, Jun. 2016, conference Name: IEEE Transactions on Computational Imaging.

[10] D. Jo, B. Yu, H. Jeon, and K. Sohn, "Image-to-Image Learning to Predict Traffic Speeds by Considering Area-Wide Spatio-Temporal Dependencies," *IEEE Transactions on Vehicular Technology*, vol. 68, no. 2, pp. 1188–1197, Feb. 2019, conference Name: IEEE Transactions on Vehicular Technology.

[11] S. Guo, Y. Lin, S. Li, Z. Chen, and H. Wan, "Deep Spatial–Temporal 3D Convolutional Neural Networks for Traffic Data Forecasting," *IEEE Transactions on Intelligent Transportation Systems*, vol. 20, no. 10, pp. 3913–3926, Oct. 2019, conference Name: IEEE Transactions on Intelligent Transportation Systems.

[12] Y. Wu, H. Tan, L. Qin, B. Ran, and Z. Jiang, "A hybrid deep learning based traffic flow prediction method and its understanding," *Transportation Research Part C: Emerging Technologies*, vol. 90, pp. 166–180, May 2018.

[13] R. de Medrano and J. L. Aznarte, "A spatio-temporal attention-based spot-forecasting framework for urban traffic prediction," *Applied Soft Computing*, vol. 96, p. 106615, Nov. 2020.

[14] Y. Li, R. Yu, C. Shahabi, and Y. Liu, "Diffusion Convolutional Recurrent Neural Network: Data-Driven Traffic Forecasting," *arXiv:1707.01926 [cs, stat]*, Feb. 2018, arXiv: 1707.01926.

[15] S. Guo, Y. Lin, N. Feng, C. Song, and H. Wan, "Attention Based Spatial-Temporal Graph Convolutional Networks for Traffic Flow Forecasting," *Proceedings of the AAAI Conference on Artificial Intelligence*, vol. 33, no. 01, pp. 922–929, Jul. 2019, number: 01.

[16] Y. Zhang and T. Cheng, "Graph deep learning model for network-based predictive hotspot mapping of sparse spatio-temporal events," *Computers, Environment and Urban Systems*, vol. 79, p. 101403, Jan. 2020.

[17] Z. Zhou and X. Li, "Graph Convolution: A High-Order and Adaptive Approach," *arXiv:1706.09916 [cs, stat]*, Oct. 2017, arXiv: 1706.09916.

[18] F. Lu, K. Liu, Y. Duan, S. Cheng, and F. Du, "Modeling the heterogeneous traffic correlations in urban road systems using traffic-enhanced community detection approach," *Physica A: Statistical Mechanics and its Applications*, vol. 501, pp. 227–237, Jul. 2018.

[19] R. Asadi and A. C. Regan, "A spatio-temporal decomposition based deep neural network for time series forecasting," *Applied Soft Computing*, vol. 87, p. 105963, Feb. 2020.

[20] P. Aram, V. Kadirkamanathan, and S. R. Anderson, "Spatiotemporal System Identification With Continuous Spatial Maps and Sparse Estimation," *IEEE Transactions on Neural Networks and Learning Systems*, vol. 26, no. 11, pp. 2978–2983, Nov. 2015, conference Name: IEEE Transactions on Neural Networks and Learning Systems.

[21] L. N. N. Do, H. L. Vu, B. Q. Vo, Z. Liu, and D. Phung, "An effective spatial-temporal attention based neural network for traffic flow prediction," *Transportation Research Part C: Emerging Technologies*, vol. 108, pp. 12–28, Nov. 2019.

[22] B. Yu, Y. Lee, and K. Sohn, "Forecasting road traffic speeds by considering area-wide spatio-temporal dependencies based on a graph convolutional neural network (GCN)," *Transportation Research Part C: Emerging Technologies*, vol. 114, pp. 189–204, May 2020.

[23] Z. Wu, S. Pan, G. Long, J. Jiang, X. Chang, and C. Zhang, "Connecting the Dots: Multivariate Time Series Forecasting with Graph Neural Networks," *KDD 2020*, May 2020, arXiv: 2005.11650.

[24] A. Uselis, M. Lukoševičius, and L. Stasytis, "Localized convolutional neural networks for geospatial wind forecasting," *arXiv:2005.05930 [cs, stat]*, May 2020, arXiv: 2005.05930.

[25] S.-I. Lee, *Correlation and Spatial Autocorrelation*. Cham: Springer International Publishing, 2017, pp. 360–368.

[26] A. D. Chouakria and P. N. Nagabhushan, "Adaptive dissimilarity index for measuring time series proximity," *Advances in Data Analysis and Classification*, vol. 1, no. 1, pp. 5–21, Feb. 2007.

[27] B. Liao, J. Zhang, C. Wu, D. McIlwraith, T. Chen, S. Yang, Y. Guo, and F. Wu, "Deep sequence learning with auxiliary information for traffic prediction," in *Proceedings of the 24th ACM SIGKDD International Conference on Knowledge Discovery and Data Mining*. ACM, 2018.

[28] Z. Cui, K. Henrickson, R. Ke, and Y. Wang, "Traffic Graph Convolutional Recurrent Neural Network: A Deep Learning Framework for Network-Scale Traffic Learning and Forecasting," *IEEE Transactions on Intelligent Transportation Systems*, pp. 1–12, 2019, conference Name: IEEE Transactions on Intelligent Transportation Systems.

[29] C. Bergmeir, R. J. Hyndman, and B. Koo, "A note on the validity of cross-validation for evaluating autoregressive time series prediction," *Computational Statistics & Data Analysis*, vol. 120, pp. 70–83, Apr. 2018.

[30] C. K. Wikle, A. Zammit-Mangion, and N. Cressie, *Spatio-Temporal Statistics with R*, 1st ed. Boca Raton, Florida : CRC Press, [2019]: Chapman and Hall/CRC, Feb. 2019. [Online]. Available: https://www.taylorfrancis.com/books/9780429649783

[31] R. Navares and J. L. Aznarte, "Predicting air quality with deep learning LSTM: Towards comprehensive models," *Ecological Informatics*, vol. 55, p. 101019, Jan. 2020.